https://dx.doi.org/10.22161/ijaers.5.12.25 ISSN: 2349-6495(P) | 2456-1908(O)

Fractional Order Butterworth Filter

Mehmet Emir Koksal

Department of Mathematics, Ondokuz Mayis University, 55139 Samsun, Turkey
Email: mekoksal@omu.edu.tr

Abstract*—Fractional order Butterworth filter derived from the conventional 3^{rd} order Butterworth filter by the transition of the ordinary derivative to the fractional one as in [1] is investigated in this paper. The change of the filter characteristics is studied depending on the order of the fractional derivative. Effects of the transformation on the components' behaviors of the filter is formulated. Design of the filter in the sense of choosing the filter parameters to satisfying the given specifications is described.*

***Keywords*—Butterworth filter, control system, fractional order.**

I. INTRODUCTION

Fractional calculus (FC) [2,3]provides more accurate models than classical calculus for many of the physical systems showing intrinsic fractional order (FO) behavior[4-6]. Fractional derivative takes into account the past history when memory like behaviors exhibit in components [7-10]. The same advantages appear in some electrical circuits as well [11-16].

In [1], a method is given for obtaining fractional order differential equation (FODE) from ordinary differential equation (ODE) keeping the consistency of dimensionality in physical systems. This method is used to find the natural response of a FO RLC circuit by F. Gomez at al. [17].

In this paper, FO Butterworth filter (FOBF) is derived by using a method similar to Gomez's method. The ordinary derivative is replaced by FO derivative) by the transformation

$$\frac{d}{dt} \to \frac{1}{\sigma^{1-\gamma}} \frac{d^{\gamma}}{dt^{\gamma}}, \qquad (1)$$

whereγ is an arbitrary parameter defining the order of derivative and the auxiliary parameter σ has the dimension of second. Time and frequency response characteristics of the obtained FOBF is investigated according to the transformation parameters $\gamma$and σ.

The paper is organized as follows: In Section 2, a brief summary of the FC relevant to the content of this paper is presented. Section 3 covers the short introduction of the conventional Butterworth filter. Section 4 describes the evaluation of the FOBF and the related formulas. In Section 5, the time and frequency domain characteristics of the FOBF is investigated. Finally, conclusions are included in Section 6.

II. FRACTIONAL CALCULUS

It is well known that Caputo fractional time derivative [16, 17] of a function $f(t)$ is defined by

$$\frac{d^{\gamma}}{dt^{\gamma}} f(t) = {}_0^C D_t^{\gamma} f(t) = \frac{1}{\Gamma(n-\gamma)} \int_0^t \frac{f^n(\tau)}{(t-\tau)^{\gamma-n+1}} d\tau \quad (2a)$$

where$\tau \in R, n-1 < \gamma \leq n \in N = \{1, 2, \dots\}$, f^n represents the ordinary derivative of order n, and Γ is the Gamma function. For $\gamma = 1$, Eq. (2) gives the usual derivative. It is assumed in the scope of this paper that t represents the time in seconds (s), and $n = 1$ so that (2) reduces to

$$\frac{d^{\gamma}}{dt^{\gamma}} f(t) = \frac{1}{\Gamma(1-\gamma)} \int_0^t \frac{f^n(\tau)}{(t-\tau)^{\gamma}} d\tau. \qquad (2b)$$

We note that Eq. (2b) yields

$$\frac{d^{\gamma}}{dt^{\gamma}} f(t)\Big|_{t=0} = \frac{1}{\Gamma(1-\gamma)} \int_0^0 \frac{f^n(\tau)}{(t-\tau)^{\gamma}} d\tau = 0. \qquad (2c)$$

Laplace transform of Eq. (2a) is

$$\mathcal{L}\left\{{}_0^C D_t^{\gamma} f(t)\right\} = s^{\gamma} F(s) - \sum_{k=0}^{n-1} s^{\gamma-k-1} f^{(k)}(0_+), n-1 < \gamma \leq n. \quad (3a)$$

For $n = 1$, that is $0 < \gamma \leq 1$,

$$\mathcal{L}\left\{{}_0^C D_t^{\gamma} f(t)\right\} = s^{\gamma} F(s) - s^{\gamma-1} f(0_+), 0 < \gamma \leq 1. \quad (3b)$$

Considering the inverse Laplace transform, a few useful formulas are listed as follows:

$$\mathcal{L}^{-1}\left\{\frac{s^{\alpha-\beta}}{s^{\alpha}-\lambda_k}\right\} = t^{\beta-1} \mathcal{E}_{\alpha,\beta}(\lambda_k t^{\alpha}). \qquad (4a)$$

Where $\mathcal{E}_{\alpha,\beta}(.)$ is the 2-parameter generalization of the Mittag-Leffler function. It is defined by

$$\mathcal{E}_{\alpha,\beta}(z) = \sum_{k=0}^{\infty} \frac{z^k}{\Gamma(\beta+\alpha k)}, \alpha, \beta, z \epsilon C; Re(\alpha) > 0, Re(\beta) > 0, \quad (4b)$$

which reduces to the original Mittag-Leffler function for $\beta = 1$:

$$\mathcal{E}_{\alpha}(z) = \mathcal{E}_{\alpha,1}(z) = \sum_{k=0}^{\infty} \frac{z^k}{\Gamma(1+\alpha k)}, \quad \alpha, z \epsilon C; Re(\alpha) > 0. \quad (4c)$$

https://dx.doi.org/10.22161/ijaers.5.12.25 ISSN: 2349-6495(P) | 2456-1908(O)

III. LOW PASS BUTTERWORTH FILTER

The transfer function of the 3rd order low pass Butterworth filter (LPBF) normalized with the $3\,dB$ cutoff frequency of $\omega_0 = 1\ r/s$ is given by

$$H(s) = \frac{1}{(s+1)(s^2+s+1)} = \frac{1}{(s^3+2s^2+2s+1)}. \quad (5a)$$

One of the circuit realizations of this transfer function is done as the voltage ratio transfer function as it is shown in Fig.1. The analysis of the circuit results the following transfer function:

$$\frac{V_R(s)}{V_S(s)} = H(s) = \frac{\frac{R}{L_1L_2C}}{s^3 + \frac{R}{L_2}s^2 + \frac{L_1+L_2}{L_1L_2C}s + \frac{R}{L_1L_2C}}. \quad (5b)$$

Equating the coefficients of the transfer functions in Eqs. (5a) and (5b) and using the normalized resistance $R = 1\ \Omega$, the following component values are obtained for the filter.

$$L_1 = 1.5\ H, L_2 = 0.5\ H, C = \frac{4}{3}F, R = 1\ \Omega. \quad (5c)$$

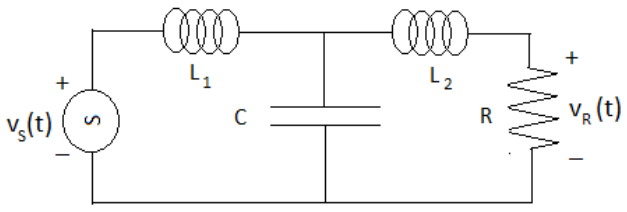

Fig.1: 3rd order Butterworth filter with $\omega_0 = 1\ r/s$.

The differential equation relating the input voltage $v_S(t)$ to the output voltage $v_R(t)$ is obtained form Eq. (5c) by inserting the Laplace operator s with the derivative operator d/dt and arranging the terms; the result is

$$\frac{d^3}{dt^3}v_R(t) + \frac{R}{L_2}\frac{d^2}{dt^2}v_R(t) + \frac{L_1+L_2}{L_1L_2C}\frac{d}{dt}v_R(t) + \frac{R}{L_1L_2C}v_R(t) = \frac{R}{L_1L_2C}v_S(t). \quad (6)$$

The frequency domain characteristics, namely gain and phase responses of the filter are obtained replacing $s\ by\ j\omega$ in Eq. (5a); the result is

$$H(j\omega) = M(\omega)e^{j\Phi(\omega)}, where \quad (7a)$$

$$M(\omega) = |H(j\omega)| = \frac{1}{\sqrt{1+\omega^6}}, \quad (7b)$$

$$\Phi(\omega) = Arg\{H(j\omega)\} = -tan^{-1}\frac{(2-\omega^2)\omega}{1-2\omega^2}, \quad (7c)$$

are the phase and phase characteristic, respectively. From Eq. (7a), it is obvious that the gain decreases from its value $1\ at\ \omega = 0$, and it becomes equal to its half power value $M = 1/\sqrt{2}\ at\ \omega = 1$, it decays to zero as $\omega \to \infty$. And the phase start from $0\ at\ \omega = 0$, it decreases monotonically to $-270^o\ as\ \omega \to \infty$. The time and frequency characteristics are not plotted at this stage since they will appear as the special case of the fractional Butterworth filter considered in the next section.

IV. FRACTIONAL ORDER LOW PASS BUTTERWORTH FILTER

Applying the fractional transformation to the components of the LPBF in Fig. 1, we have the following time and Laplace domain element behavior equations in the circuit:

$$v_R(t) = Ri_R(t), \quad V_R(s) = RI_R(s), \quad (8a)$$

$$v_{L_i}(t) = L_i\frac{1}{\sigma^{1-\gamma}}\frac{d^\gamma i_L(t)}{dt^\gamma}, V_{L_i}(s) = L_i\frac{1}{\sigma^{1-\gamma}}s^\gamma I_{L_i}(s), i = 1,2, \quad (8b)$$

$$i_C(t) = C\frac{1}{\sigma^{1-\gamma}}\frac{d^\gamma v_C(t)}{dt^\gamma}, I_C(s) = C\frac{1}{\sigma^{1-\gamma}}s^\gamma V_C(s). \quad (8c)$$

The frequency and time domain analysis of the circuit with these component behavior equations, or direct substitutions $s \to \frac{s^\gamma}{\sigma^{1-\gamma}}$ in Eq. (5b) and $\frac{d}{dt} \to \frac{1}{\sigma^{1-\gamma}}\frac{d^\gamma}{dt^\gamma}, \frac{d^2}{dt^2} \to \frac{1}{\sigma^{2(1-\gamma)}}\frac{d^{2\gamma}}{dt^{2\gamma}}, \frac{d^3}{dt^3} \to \frac{1}{\sigma^{3(1-\gamma)}}\frac{d^{3\gamma}}{dt^{3\gamma}}$, in Eq. (6) yield

$$\frac{V_R(s)}{V_S(s)} = H(s) = \frac{\frac{R\sigma^{3(1-\gamma)}}{L_1L_2C}}{s^{3\gamma} + \frac{R\sigma^{(1-\gamma)}}{L_2}s^{2\gamma} + \frac{(L_1+L_2)\sigma^{2(1-\gamma)}}{L_1L_2C}s^\gamma + \frac{R\sigma^{3(1-\gamma)}}{L_1L_2C}}, \quad (9a)$$

$$\frac{d^{3\gamma}}{dt^{3\gamma}}v_R(t) + \frac{R\sigma^{(1-\gamma)}}{L_2}\frac{d^{2\gamma}}{dt^{2\gamma}}v_R(t) + \frac{(L_1+L_2)\sigma^{2(1-\gamma)}}{L_1L_2C}\frac{d^\gamma}{dt^\gamma}v_R(t) + \frac{R\sigma^{3(1-\gamma)}}{L_1L_2C}v_R(t) = \frac{R\sigma^{3(1-\gamma)}}{L_1L_2C}v_S(t). \quad (9b)$$

respectively. The characteristic equation is obtained by equating the denominator polynomial of the transfer function in Eq. (9a) to zero:

$$s^{3\gamma} + \frac{R\sigma^{(1-\gamma)}}{L_2}s^{2\gamma} + \frac{(L_1+L_2)\sigma^{2(1-\gamma)}}{L_1L_2C}s^\gamma + \frac{R\sigma^{3(1-\gamma)}}{L_1L_2C} = 0. \quad (9c)$$

The characteristic polynomial appearing in the left side of the equality in Eq. (9c) is s a commensurate polynomial in power s^γ. So the time domain responses (such as step and impulse responses) of the filter can be obtained analytically by using Mittag-Leffler function [5]. But, these solutions are not included within the content of the paper and it is satisfied by their plots only, instead we are confined to the frequency domain responses.

V. FILTER CHARACTERISTICS

To find the gain and phase characteristics of the FO LPBF derived in the previous section, we let $s = j\omega$ in Eq. (9a) and use the identity

https://dx.doi.org/10.22161/ijaers.5.12.25 *ISSN: 2349-6495(P) | 2456-1908(O)*

$$(j\omega)^{\gamma} = \omega^{\gamma}\left(e^{j\frac{\pi}{2}}\right)^{\gamma} = \omega^{\gamma}e^{j\frac{\pi}{2}\gamma}$$
$$= \omega^{\gamma}\left[\cos\left(\frac{\pi}{2}\gamma\right) + j\sin\left(\frac{\pi}{2}\gamma\right)\right]. \quad (10)$$

The result is

$$M(\omega) = \frac{b_0}{\sqrt{A^2 + B^2}}, \quad (11a)$$
$$\Phi(\omega) = -Arctan\left(\frac{B}{A}\right), \quad (11b)$$

where

$$A = \omega^{3\gamma}\cos(1.5\pi\gamma) + a_2\omega^{2\gamma}\cos(\pi\gamma) + a_1\omega^{\gamma}\cos(0.5\pi\gamma) + a_0, \quad (11c)$$
$$B = \omega^{3\gamma}\sin(1.5\pi\gamma) + a_2\omega^{2\gamma}\cos(\pi\gamma) + a_1\omega^{\gamma}\cos(0.5\pi\gamma), \quad (11d)$$
$$a_2 = \frac{R\sigma^{(1-\gamma)}}{L_2}, \quad a_1 = \frac{(L_1+L_2)\sigma^{2(1-\gamma)}}{L_1L_2C}, \quad (11e,f)$$
$$a_0 = b_0 = \frac{R\sigma^{3(1-\gamma)}}{L_1L_2C}. \quad (11g,h)$$

The gain and phase characteristics on the logarithmic scale (Bode plots) of the filter for $\sigma = 1$ and different values of γ is shown in Fig. 2 where the conventional 3rd order Butterworth filter characteristics is shown by the thick dashed red line ($\gamma = 1$); The details of the numerical data is given in Table 1 where M_p (in dB) is the peak gain at the peak frequency ω_p (in rad/s) , $M_1 = M_2 = M_p - 3$are the gains at the cut off frequencies ω_1 and ω_2, BW is the bandwidth which is defined as $\omega_2 - \omega_1$ if a peak exist (the case $\gamma = 1$); otherwise $BW = \omega_2$ (the cases $\gamma = 1, 0.75, 0.50$) The quality factor $Q = \omega_2/(\omega_2 - \omega_1)$is defined only for $\gamma = 1.25$ for which the gain characteristics has a peak exceeding the 0 dB level and the filter can be considered as of bandpass type as well. It is observed from Fig. 2 and the data given in Table 1 that the first cut off frequency ω_1 and the associated gain M_1, and Q are defined only when the characteristic is handled as a BP type for which BW=0.221. In general, the bandwidth (BW) and hence the cut off frequency ($\omega_2 = BW$) decreases with decreasing γ values for the LP filter.

The phase characteristics decrease from 0^o *to* -180^o as $\omega: 0 \to \infty$ but with a faster rate at the intermediate frequencies with increasing γ.

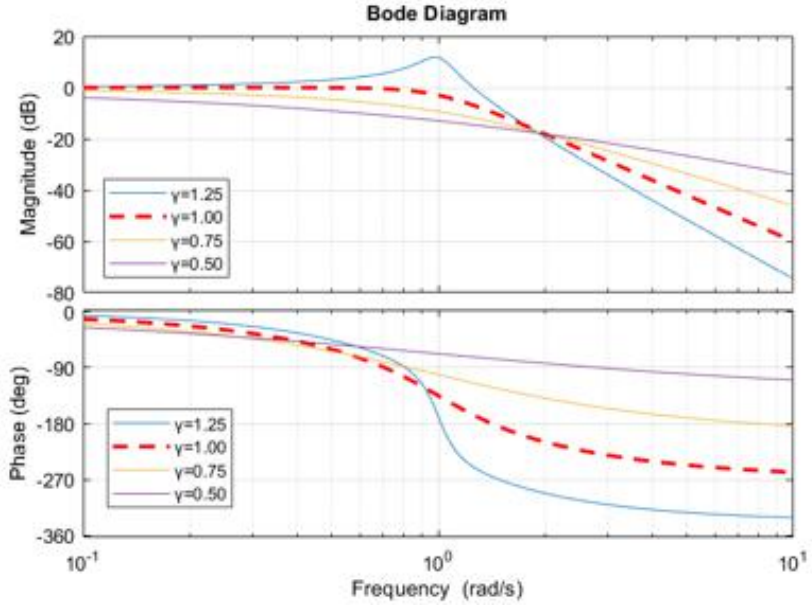

Fig.2: Bode plots of the transfer function for σ =1.00.

Table.1: Numerical data for frequency response curves when $\sigma = 1$ for the filter.

γ	$\omega_1 - (M_1)$	$\omega_2 - (M_2)$	$\omega_p - (M_p)$	$BW - (BP)$	$Q - BP$
1.25	0.852 - 8.841	1.073 - 8.867	0.979 – (11.844)	1.073 – (0.221)	4.430
1.00	---	1.000 – (-3)	0 – (0)	1.000 – (---)	---
0.75	---	0.313 – (-3)	0 – (0)	0.313 – (---)	---
0.50	---	0.058 – (-3)	0 – (0)	0.058 – (---)	---

The step response of the filter is shown in Fig. 3 for values of $= 1.25, 1.00, 0.75, 0.50$. It is seen that all the responses start from $0\ at\ t = 0$ and approaches to $\infty\ as\ t \to \infty$, which is a typical property for a LP filter. The response is highly oscillatory for $\gamma = 1.25$, the case in which the filter can be interpreted as a BP filter as well. There is a smaller overshoot for the ordinary 3rd order Butterworth filter (case $\gamma = 1.00$, thick red dashed line).

https://dx.doi.org/10.22161/ijaers.5.12.25 *ISSN: 2349-6495(P) | 2456-1908(O)*

The rise time and the settling time decreases as γ takes smaller values. See Table 2 for the detailed numerical data, where T_r: rise time, T_r: rise time, T_{p1}, T_{p2}, T_{p3}: peak times, M_{p1}, M, M_{p3}: peak values, T_s: settling time all in seconds. Some of the data could not be detected since the simulations are done up to 40 s. Rise time increases with decreasingγ and the minimum settling time occurs for the conventional filter (γ).

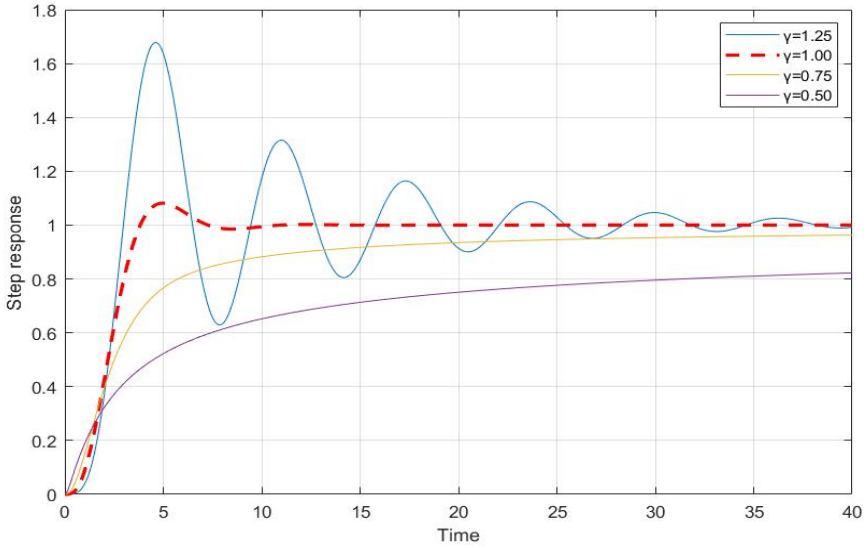

Fig.3: Step responses of the transfer function when σ =1.00.

Table.2: Step response characteristics for σ =1.00.

γ	T_r	$T_{p1} - M_{p1}$	$T_{p2} - M_{p2}$	$T_{p3} - M_{p3}$	T_s
1.25	1.49	4.56 - 1.678	10.95 - 1.315	17.27 - 1.634	24.63
1.00	2.29	4.93 – 1.082	12.10 – 1.002	-----	5.98
0.75	11.25	-----	-----	-----	27.51
0.50	-----	-----	-----	-----	-----

Similar characteristics for $\sigma = 0.1$ and the same different values of γ considered before are presented in Fig. 4 and Table 3. The general arguments discussed for the case $\sigma = 1$ hold. For $\gamma = 1.25$, all the critical frequencies are increased whilst the critical gains and the quality factor remain the same. For $\gamma = 1.00$ the responses are hardly affected. For $\gamma \leq 1$, all the critical frequencies decrease with decreasing γ.

Considering the phase characteristic, it is slightly increased (decreased) for $\gamma = 1.25$ ($\gamma < 1.00$) and almost unaffected for $\gamma = 1.00$.

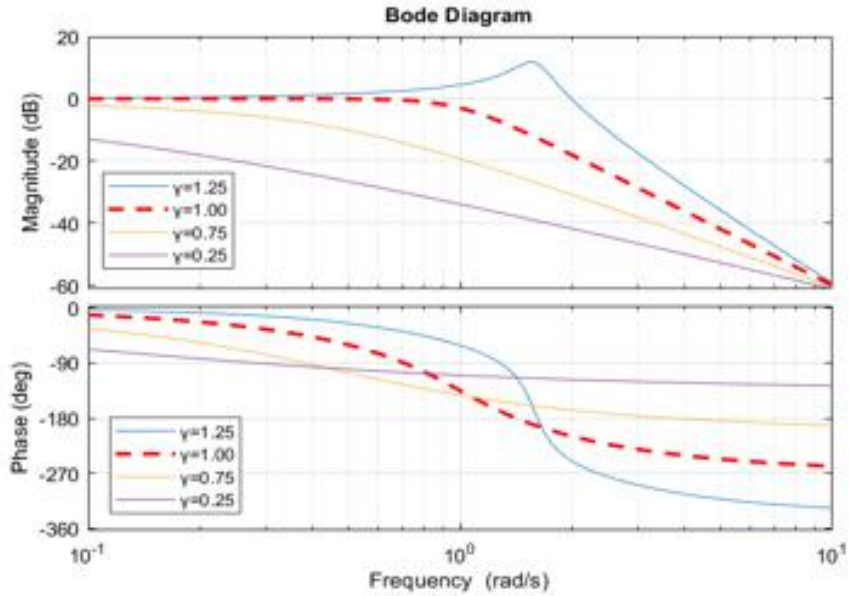

Fig.4: Bode plots of the transfer function for σ =0.1.

https://dx.doi.org/10.22161/ijaers.5.12.25 *ISSN: 2349-6495(P) | 2456-1908(O)*

Table.3: Numerical data for frequency response curves when $\sigma = 0.1$ for the filter.

γ	$\omega_1 - (M_1)$	$\omega_2 - (M_2)$	$\omega_p - (M_p)$	$BW - (BP)$	$Q - BP$
1.25	1.350 - 8.835	1.701 - 8.854	1.552 – (11.844)	1.701 – (0.351)	4.422
1.00	---	1.000 – (-3)	0 – (0)	1.000 – (---)	---
0.75	---	0.145 – (-3)	0 – (0)	0.145 – (---)	---
0.50	---	0.006 – (-3)	0 – (0)	0.006 – (---)	---

Step response of the filter for $\sigma = 0.1$ is shown in Fig. 5. It is seen that the conventional Butterworth filter response is not affected by σ when $\gamma = 1.00$ (see the legends $\gamma = 1.25$ *and* $\gamma = 1.25*$). Further, the peak values of oscillations are not affected by changing $\sigma$from 1 *to* 0.1. But there is an apparent time lead (squeeze) for $\gamma = 1.25 >$, and time lag (spread) for $\gamma = 0.75 < 1$. The lag (spread) is higher for $\gamma = 0.50$. See Table 4 for numerical details. The time lead (lag) is used in the sense of faster (slower) motion.

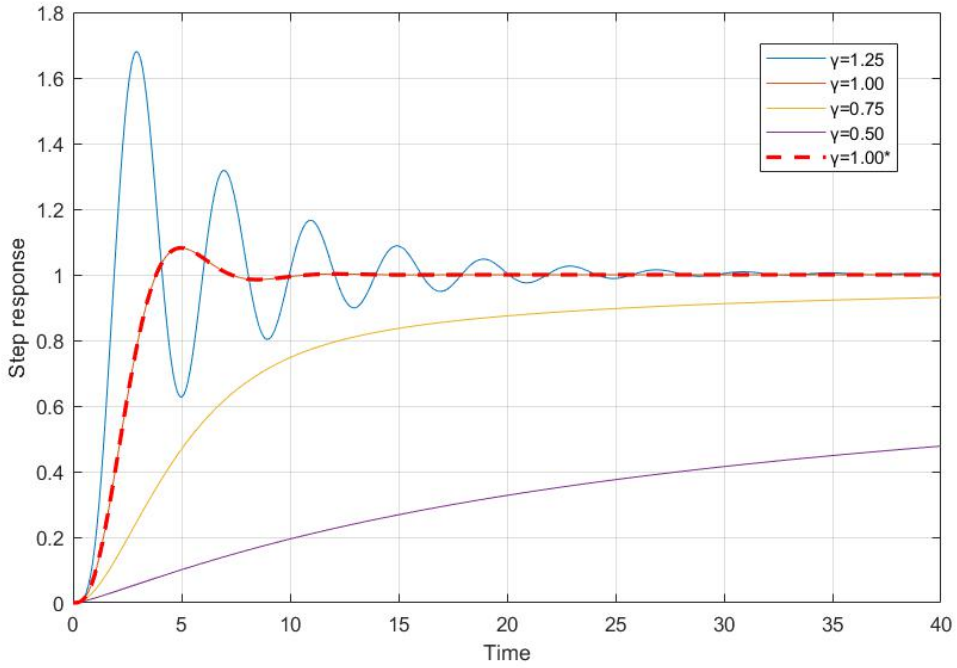

Fig.5: Step responses of the transfer function when σ =0.1.

Table 4: Step response characteristics for σ =0.1.

γ	T_r	$T_{p1} - M_{p1}$	$T_{p2} - M_{p2}$	$T_{p3} - M_{p3}$	T_s
1.25	1.49	2.88 - 1.678	6.91 - 1.315	10.90 - 1.634	15.54
1.00	2.29	4.93 – 1.082	12.10 – 1.002	19.35 – 1.000	5.98
0.75	24.24	-----	-----	-----	-----
0.50	-----	-----	-----	-----	-----

Similar frequency characteristics for $\sigma = 10$ and the same different values of γ considered before are presented in Fig. 2 and Table 1. The general arguments discussed for the case $\sigma = 1$ hold. For $\gamma = 1.25$, all the critical frequencies are decreased whilst the critical gains and the quality factor remain almost the same. For $\gamma = 1.00$ the responses are hardly affected. For $\gamma \leq 1$, all the critical frequencies decrease with decreasing γ.

Considering the phase characteristic, it is decreased (increased) for $\gamma = 1.25$ $(\gamma < 1.00)$ and almost unaffected for $\gamma = 1.00$.

https://dx.doi.org/10.22161/ijaers.5.12.25 *ISSN: 2349-6495(P) | 2456-1908(O)*

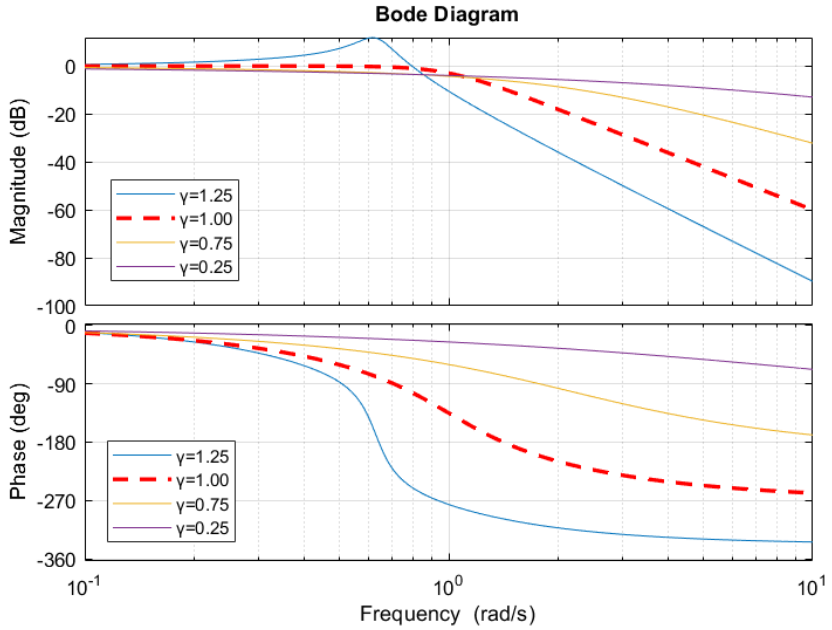

Fig.6: Bode plots of the transfer function for σ =10.

Table.5: Numerical data for frequency response curves when $\sigma = 10$ for the filter.

γ	$\omega_1 - (M_1)$	$\omega_2 - (M_2)$	$\omega_p - (M_p)$	$BW - (BP)$	$Q - BP$
1.25	0.537 - 8.815	0.677 - 8.868	0.618 – (11.844)	0.677 – (0.140)	4.414
1.00	---	1.000 – (-3)	0 – (0)	1.000 – (---)	---
0.75	---	0.145 – (-3)	0 – (0)	0.145 – (---)	---
0.50	---	0.006 – (-3)	0 – (0)	0.006 – (---)	---

Step response of the filter for $\sigma = 10$ is shown in Fig. 5. It is seen that the conventional Butterworth filter response is not affected by σ when $\gamma = 1.00$ (see the legends $\gamma = 1.25$ *and* $\gamma = 1.25*$). Further, the peak values of oscillations are not affected by changing σ from 1 to 10. But there is an apparent time lag (spread) for $\gamma = 1.25 > 1$, and time lead (squeeze) for $\gamma = 0.75 < 1$. The lead (squeeze) is higher for $\gamma = 0.50$.

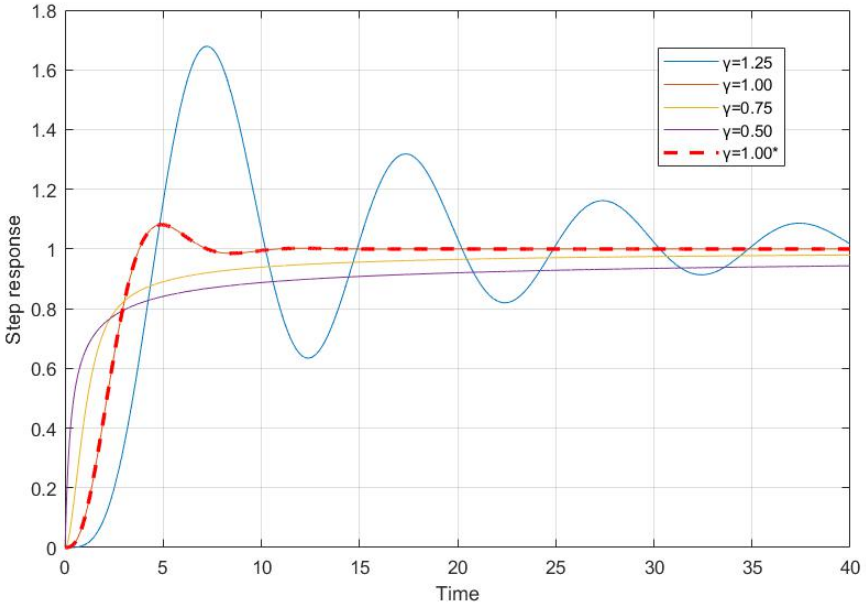

Fig.7: Step responses of the transfer function when σ =10.

https://dx.doi.org/10.22161/ijaers.5.12.25 *ISSN: 2349-6495(P) | 2456-1908(O)*

Table.6: Step response characteristics for σ =10.

γ	T_r	$T_{p1} - M_{p1}$	$T_{p2} - M_{p2}$	$T_{p3} - M_{p3}$	T_s
1.25	2.38	7.23 - 1.678	17.35 - 1.315	27.37 - 1.634	39.05
1.00	2.29	4.93 – 1.082	12.10 – 1.002	19.35 – 1.000	5.98
0.75	5.22	-----	-----	-----	12.77
0.50	12.63	-----	-----	-----	-----

VI. CONCLUSION

A FO Butterworth filter derived from the conventional 3rd order Butterworth filter by the IO derivative to FO derivative transformation with two parameters γ *and* σ as in [17] is investigated in this paper. It is arrived the following conclusions.

1. A variety of low pass filters can be obtained by changing the parameters $\gamma$and σ.
2. For $\gamma > 1$, the classical frequency response curve of the Butterworth filter disappears, and a peak occur in the frequency response.
3. When $\gamma = 1$, σ does not effect on the characteristics.
4. σdominantly affect the time characteristics, critical magnitudes of the time responses are not changed, but increase of σ cuuses a slower (faster) response for $\gamma > 1$ ($\gamma < 1$). That is σ effects like a time scaling operator.
5. Effect of σ on the phase characteristics is that increase of σ decreases (increases the phase if $\gamma > 1$ ($\gamma < 1$).
6. For $\gamma > 1$ and as $\gamma \to 1.38$ the filter can be used a high-Q narrow band pass filter as well. But in the limit case the filter becomes unstable.

Having in mind these conclusions, fractional order low pass filters and/or band pass filers can be designed.

REFERENCES

[1] J.F. Gomez-Aguilar, J.J. Rosales-Garcia, J.J. Bernal-Alvarado, et al., "Fractional mechanical oscillators", Revista Mexicana de Fisica, vol. 58, pp. 348–352, 2012.

[2] K. Diethelm, D. Baleanu, E. Scalas, J.J. Trujillo, "Fractional Calculus: Models and Numerical Methods", 2 Ed., Singapore: World Scientific, 2016.

[3] I. Podlubny, "Fractional Differential Equations", vol. 198, Academic Press, Boston, 1999.

[4] S. Zheng, W. Li, "Robust stabilization of fractional-order plant with general interval uncertainties based on graphical method", International Journal of Robust and Nonlinear Control, vol. 28, pp. 1672-1692, 2018.

[5] A Pratap, R Raja, C Sowmiya, et all. "Robust generalized Mittag-Leffler synchronization of fractional order neural networks with discontinuous activation and impulses", Neural Networks, vol. 103, pp. 128-141, 2018.

[6] V.A. Vyawahare, G. Espinosa-Paredes, "On the stability of linear fractional-space neutron point kinetics (F-SNPK) models for nuclear reactor dynamics",Annals of Nuclear Energy,vol. 111, pp. 12–21, 2018.

[7] A. Karthikeyan, K. Rajagopal ,"FPGA implementation of fractional-order discretememristor chaotic system and its commensurate and incommensurate synchronizations", J. Phys., vol. 90, pp. 1-13, 2018.

[8] A.A. Kilbas, H.M. Srivastava, J. J. Trujillo, "Theory and Applications of Fractional Differential Equations", North-Holland Mathematical Studies, Vol. 204, Elsevier, Amsterdam, 2006.

[9] J. Ma, P. Zhou, B. Ahmad, et. all, "Chaos and multi-scroll attractors in RCL-shunted junction coupled Jerk circuit connected by memristor", PloS One, vol. 13, pp. 1-21, 2018.

[10] S. Bhalekar, V. Daftardar-Gejji, D. Baleanu, R. Magin, "Transient chaos in fractional Bloch equations, Computers and Mathematics with Applications", vol. 64, pp. 3367-3376, 2012.

[11] J. Dvorak, L. Langhammer, at. all, "Synthesis and analysis of electronically adjustable fractional-order low-pass filter", Journal of Circuits, Systems and Computers,vol. 27, DOI: S0218126618500329,2018.

[12] J. Dvorak, Z. Polesakova, at. all, "Non-Integer-Order Low-Pass Filter with Electronically Controllable Parameters", IEEE-Xplore, DOI: 978-1-5386-4881-0/18, 2018.

[13] G. Liang, Y. Jing, at. all, "Passive synthesis of a class of fractional immittance function based on multivariable theory", Journal of Circuits, Systems and Computers, vol. 27, DOI: 10.1142/S0218126618500743, 2018.

[14] A. Agambayev, K.H. Rajab, Towards fractional-order capacitors with broad tunable constant phase angles: multi-walled carbon nanotube-polymer composite as a case study, Journal of Physics D: Applied Physics,vol.51, pp. 1-6, 2018

[15] A. Jakubowska-Ciszek, J. Walczak, "Analysis of the transient state in a parallel circuit of the class

https://dx.doi.org/10.22161/ijaers.5.12.25 *ISSN: 2349-6495(P) | 2456-1908(O)*

RLβC$^{\alpha}$", Applied Mathematics and Computation, vol. 319, pp. 287-300, 2018.

[16] P. Bertsias, C. Psychallions, at. all, "Differentiator based fractional-order high-pass filter designs", Proceedings of the 7th International Conference on Modern Circuits and Systems Technologies (MOCAST), Article ID: 17840792, 2018.

[17] F. Gomez, J. Rosales, M. Guia, "RLC electrical circuits of non-integer order", Central European Journal of Physics, vol. 11, pp. 1361-1365, 2013.